FA oxidation, and liver tumors. Thus, AOX deficiency results in inflammation, cell proliferation, and carcinogenesis in the liver [86]. However, this model apparently does not develop fibrosis despite exhibiting liver tumors.

3.3.3. PPARα-Deficient Mice

Peroxisomes catalyze fatty acid β-oxidation. Mice with a homozygous knockout of PPARα (peroxisome proliferator activated receptor alpha), which is a member of the steroid/nuclear receptor superfamily and mediates the biological and toxicological effects of peroxisome proliferators, do not accumulate fat under normal feeding conditions but fail to up-regulate FA oxidation, and thus develop severe steatosis when fatty acid delivery to the liver is increased by fasting [87].

3.3.4. Other Models of Reduced Oxidation

The involvement of estrogens in the regulation of carbohydrate and lipid metabolism has been robustly demonstrated by studies in genetically engineered mice, including aromatase knockout mice lacking intrinsic estrogen production. The oxidation of FA under normal physiological conditions may be orchestrated by an estrogen receptor-mediated signaling pathway. Aromatase knockout mice exhibit hyperinsulinemia and steatosis without inflammation [88].

Juvenile visceral steatosis (JVS) mice are an animal model of systemic carnitine deficiency with a genetic defect in organic cation transporter 2 (*OCTN2*). The abnormalities in this strain may be caused by the accumulation of long-chain fatty acids, which are not well metabolized as a result of their disturbed entry into mitochondria in carnitine-deficient states. These mice suffer from steatosis without inflammation, hypoglycemia, hyperammonemia, growth retardation, and cardiac hypertrophy [89].

Neonatal hepatic steatosis is a fatal condition of unknown etiology. A deficit in adenosine-dependent metabolism has been proposed as a possible causative factor. Physiologically, adenosine is efficiently metabolized to AMP by adenosine kinase (ADK), an enzyme that is highly expressed in the liver. ADK not only ensures normal adenine nucleotide levels but also is essential for the maintenance of *S*-adenosylmethionine-dependent transmethylation processes, from which adenosine, an obligatory product, has to be constantly removed. ADK knockout mice develop neonatal hepatic steatosis without inflammation, providing a powerful model for the rapid development of postnatally lethal fatty liver [90].

Cystathionine beta-synthase (CBS) is subject to complex regulation, including allosteric activation by the methyl donor *S*-adenosylmethionine (AdoMet). CBS is the rate-limiting enzyme of the transsulfuration pathway, which condenses homocysteine and serine into cystathionine. CBS knockout mice develop not only steatosis but also inflammation and fibrosis concomitant with an enhanced expression of proinflammatory cytokines [91].

Chow-fed female mice with a truncating mutation (*foz*) in the Alstrom syndrome 1 (*ALMS1*) gene, exhibit disordered appetite regulation and develop obesity, diabetes, and simple steatosis. In addition, HFD-fed *foz/foz* mice exhibit severe steatohepatitis, such as lobular inflammatory infiltrate and pericellular fibrosis, through the inhibition of PPARα-mediated peroxisomal FA oxidation via hypoadiponectinemia [92].

3.4. Models with Reduced VLDL Secretion

Triglycerides (TG) are bound by apolipoprotein B (ApoB) and build up into a mature lipoprotein particle that is then secreted [91]. ApoB synthesis is stimulated by elevated levels of FA and TG, as well as by microsomal triglyceride transfer protein (MTP), and is inhibited by insulin [93,94]. Thus, in the presence of an elevated FA afflux to the liver and normal/decreased insulin concentrations or IR, the secretion of mature VLDL-ApoB is expected to increase. The bulk of TG incorporated into VLDL originates from intracellular storage pools rather than from de novo synthesis [94]. The balance between the FA and insulin effects, determines whether the TG are combined with the ApoB VLDL particles and secreted or, alternatively, retained within the liver. Under the condition of IR, despite increased FA levels, TG are maintained within the liver, thus inducing steatosis. This key step may be relevant to the pathogenesis of NAFLD. In fact, the level of serum TG in secreted VLDL reportedly decreased as the MTP mRNA level decreased in human NASH patients [95].

3.4.1. Mice Fed a MCD Diet

Mice fed a MCD diet are a frequently used nutritional model of NASH, that induces an elevation in aminotransferase and hepatic histological changes characterized by steatosis, focal inflammation, hepatocyte necrosis, and fibrosis [96]. Previous studies, using a choline-deficient (methionine-containing) diet, suggest that the pathogenesis of hepatic steatosis may be attributable, at least in part, to impairment in hepatic VLDL secretion. This assumption is further supported by the fact that methionine and choline are precursors to phosphatidylcholine, the main phospholipid coating VLDL particles. Thus, impaired VLDL secretion may play a role in MCD diet-induced hepatic lipid accumulation in mice. However, this model does not exhibit increased FA, obesity, or IR, which are recognized features of human NASH.

3.4.2. Hepatocyte-Specific MTP-Deficient Mice

Microsomal triglyceride transfer protein (MTP) is required for the secretion of ApoB-containing lipoproteins from hepatocytes and from the absorptive enterocytes of the intestine. MTP is located within the lumen of the endoplasmic reticulum (ER), where it is assumed to transfer lipids during the assembly of lipoproteins. Hepatocyte-specific MTP knockout mice exhibit moderate hepatic steatosis without inflammation when fed a low-fat diet [97].

3.4.3. PITPα-Deficient Mice

Phosphatidylinositol transfer proteins (PITPs) regulate the interface between lipid metabolism and cellular functions [98]. PITPα knockout mice develop aponecrotic spinocerebellar disease, hypoglycemia, and intestinal and hepatic steatosis without inflammation [99].

3.4.4. Other Models of Reduced VLDL Secretion

Phosphatidylcholine, which is produced by the methylation of phosphatidylethanolamine using *S*-adenosylmethionine in a reaction that is catalyzed by phosphatidylethanolamine *N*-methyltransferase (PEMT), is a significant component of biomembranes and is required for the formation of the VLDL

particle. PEMT knockout mice exhibit steatosis partly because VLDL cannot be exported from the liver [100]. Fibrosis does not seem to occur in this model.

Apolipoprotein E (ApoE) is a structural component of all lipoprotein particles except for LDL and serves as a high-affinity ligand for lipoprotein receptors. ApoE plays important roles in the hepatic uptake of chylomicron and VLDL remnants as well as in the hepatic secretion of VLDL [101]. ApoE knockout mice fed normal chow exhibit only steatosis but are characterized by the appearance of inflammatory cell infiltration with casein, inducing a predictable low-grade, systemic inflammation [102]. Moreover, ApoE knockout mice fed a HFD are characterized by the development of histological steatohepatitis.

3.5. Models with Increased Hepatic Cholesterol

Hepatic cholesterol accumulates when its dietary intake increases or its elimination decreases. The primary route of cholesterol elimination from the body is via the bile through both the direct canalicular excretion of biliary cholesterol and the conversion of hepatic cholesterol to bile acids [103]. Hepatic cholesterol accumulation leads to calcium depletion and endoplasmic reticulum (ER) stress with the activation of the unfolded protein response and ER stress-induced apoptosis. Moreover, hepatic cholesterol accumulation may reduce mitochondrial glutathione stores and could be corrected by *S*-adenosyl-L-methionine, which replenishes the mitochondrial glutathione levels [104,105]. Analyses of the lipid composition of human liver samples demonstrate a progressive increase in hepatic cholesterol content in subjects with NAFLD or with NASH [106]. CD36 and macrophage scavenger receptor 1 (MSR1), which are main scavenger receptors and important for modified cholesterol-rich lipoprotein uptake, have been shown to contribute independently to the onset of inflammation in NAFLD, by affecting intracellular cholesterol distribution [107]. These results suggest that disordered cholesterol metabolism may be associated with NAFLD.

3.5.1. IL-1 Ra-Deficient Mice

Interleukin 1 (IL-1) is a pro-inflammatory cytokine that plays important roles in inflammation. However, IL-1 is also involved in peripheral energy homeostasis through endocrine mechanisms that are involved in cholesterol metabolism. IL-1 receptor antagonists (IL-1 Ra) prevent the effects of IL-1. IL-1 Ra knockout mice exhibited severe steatosis and pericellular fibrosis containing many inflammatory cells, similar to the situation in human NASH, following 20 weeks of feeding with an atherogenic diet [108].

3.5.2. Rabbit Fed a High-Fat and High-Cholesterol Diet

Japanese white rabbits fed a high-fat and high-cholesterol diet may be a good model of human NASH because these animals develop obesity, hyperinsulinemia, hyperglycemia, hypertension, hepatic inflammatory cell infiltration, and even hepatic fibrosis [109].

3.6. Model with Endotoxin-Induced Liver Inflammation

Chronic inflammation is an important contributing factor in NASH pathogenesis [110]. As a major outer membrane constituent of gram-negative bacteria, lipopolysaccharide (LPS), also referred to as

endotoxin, is considered a potent inducer of hepatic inflammation. LPS may be capable of stimulating inflammation, cytokine production, and accumulation of inflammatory cells within the liver. In fact, LPS has been reported to be the predominant cause of liver neutrophil infiltration in NASH patients [111]. In addition, several previous reports have shown that gut permeability, or small intestinal bacterial overgrowth, was observed more frequently in NASH patients than in healthy control subjects [112]. Interestingly, p53, a tumor suppressor protein that regulates the cell cycle, is reported to be involved in the molecular mechanisms of hepatocellular injury associated with NAFLD via endotoin-induced liver inflammation [113].

3.6.1. Mice with Intraperitoneal Injection of Low-Dose LPS

Gut-derived bacterial endotoxin may play a role in the progression of disease from simple steatosis to steatohepatitis in NASH [114]. A previous study showed that the responsivity to low-dose LPS was enhanced in HFD-induced murine steatosis, and that low-dose LPS led to liver injury and severe hepatic fibrosis in HFD-fed mice, but not in chow-fed mice [115]. In addition, obesity-induced leptin induces the overexpression of CD14 via activation of STAT3 signaling in Kupffer cells, resulting in a hepatic hyper inflammatory response to low-dose LPS, and plays a crucial role in the progression of NASH [115]. This low-dose LPS-induced NASH model exhibits increased FA levels, obesity, IR, inflammation, and fibrosis, but not carcinoma.

4. Conclusions

NAFLD, including NASH, likely represents the tip of the iceberg of several complex biochemical, metabolic, and clinical conditions. Despite the well-defined morphological features of these conditions, our knowledge regarding the pathogenetic mechanisms and appropriate therapeutic approaches remains mostly lacking. Rodent models are essential tools for studies of disease pathogenesis. Ideally, rodent models should not only reproduce the established pathology of the human disease but also reenact the context within which the disease develops and progresses, as described above. However, rodent models of NAFLD/NASH have a number of problems, as described below. First, some features of true steatohepatitis such as ballooning hepatocyte degeneration, in addition to simple fatty changes and inflammatory infiltrates [5,110–113], are rarely demonstrated in rodent models of NAFLD/NASH; Second, no existing model exhibits cardiovascular disease, which is the most common cause of death among NAFLD/NASH patients; Third, models with genetic alterations may not reflect human NAFLD/NASH appropriately. Thus, no existing model reproduces the complete NAFLD/NASH phenotype as encountered in clinical practice, and many of the models differ from the human disease in all but the gross histological appearance. These inconsistencies and the lack of a reliable model for progressive fibrosing steatohepatitis have hampered research in this field. However, if each of the available rodent models described in this article are used appropriately, the pathogenesis of this condition may be clarified. To develop an ideal model of NAFLD/NASH, scientists should continue to improve on the current models and to develop novel models. In doing so, scientists should be able to facilitate the advancement of knowledge on the disease's pathogenesis, eventually leading to a full understanding of human NAFLD/NASH and the development of effective therapies for this condition.

Acknowledgments

The skillful technical assistance of Machiko Hiraga, Ayaka Miura, and Tamiyo Taniguchi are gratefully acknowledged. All authors read and approved the final manuscript.

Conflicts of Interest

The authors declare no conflict of interest.

References

1. Sanyal, A.J. AGA technical review on nonalcoholic fatty liver disease. *Gastroenterology* **2002**, *123*, 1705–1725.
2. Marchesini, G.; Bugianesi, E.; Forlani, G.; Cerrelli, F.; Lenzi, M.; Manini, R.; Natale, S.; Vanni, E.; Villanova, N.; Melchionda, N.; *et al.* Nonalcoholic fatty liver, steatohepatitis, and the metabolic syndrome. *Hepatology* **2003**, *37*, 917–923.
3. Angulo, P. Nonalcoholic fatty liver disease. *N. Engl. J. Med.* **2002**, *346*, 1221–1231.
4. Clark, J.M.; Brancati, F.L.; Diehl, A.M. Nonalcoholic fatty liver disease. *Gastroenterology* **2002**, *122*, 1649–1657.
5. Neuschwander-Tetri, B.A.; Caldwell, S.H. Nonalcoholic steatohepatitis, summary of an AASLD single topic conference. *Hepatology* **2003**, *37*, 1202–1219.
6. Day, C.P. Non-alcoholic steatohepatitis (NASH), where are we now and where are we going? *Gut* **2002**, *50*, 585–588.
7. Fan, J.-G.; Li, F.; Cai, X.-B.; Peng, Y.-D.; Ao, Q.-H.; Gao, Y. Effects of nonalcoholic fatty liver disease on the development of metabolic disorders. *J. Gastroenterol. Hepatol.* **2007**, *22*, 1086–1091.
8. Harrison, S.A.; Torgerson, S.; Hayashi, P.H. The natural history of nonalcoholic fatty liver disease, a clinical histopathological study. *Am. J. Gastroenterol.* **2003**, *98*, 2042–2047.
9. Day, C.P.; Saksena, S. Non-alcoholic steatohepatitis, definitions and pathogenesis. *J. Gastroenterol. Hepatol.* **2002**, *17*, 377–384.
10. Powell, E.E.; Cooksley, W.G.; Hanson, R.; Searle, J.; Halliday, J.W.; Powell, L.W. The natural history of nonalcoholic steatohepatitis, a follow-up study of forty-two patients for up to 21 years. *Hepatology* **1990**, *11*, 74–80.
11. Day, C.P.; James, O.F. Steatohepatitis, a tale of two "hits"? *Gastroenterology* **1998**, *114*, 842–845.
12. Tilg, H.; Moschen, A.R. Evolution of inflammation in nonalcoholic fatty liver disease: The multiple parallel hits hypothesis. *Hepatology* **2010**, *52*, 1836–1846.
13. Day, C.P. Pathogensis of steatohepatitis. *Best Pract. Res. Clin. Gastroenterol.* **2002**, *16*, 663–678.
14. London, R.M.; George, J. Pathogenesis of NASH, animal models. *Clin. Liver Dis.* **2007**, *11*, 55–74.
15. Wanless, I.R.; Shiota, K. The pathogenesis of nonalcoholic steatohepatitis and other fatty liver diseases, a four-step model including the role of lipid release and hepatic venular obstruction in the progression to cirrhosis. *Semin. Liver Dis.* **2004**, *24*, 99–106.
16. Farrell, G.C.; Larter, C.Z. Nonalcoholic fatty liver disease, from steatosis to cirrhosis. *Hepatology* **2006**, *43*, 99–112.

17. Cohen, J.C.; Horton, J.D.; Hobbs, H.H. Human fatty liver disease: Old questions and new insights. *Science* **2011**, *332*, 1519–1523.
18. Fan, J.G.; Xu, Z.J.; Wang, G.L. Effect of lactulose on establishment of a rat non-alcoholic steatohepatitis model. *World J. Gastroenterol.* **2005**, *11*, 5053–5056.
19. Larter, C.Z. Not all models of fatty liver are created equal, understanding mechanisms of steatosis development is important. *J. Gastroenterol. Hepatol.* **2007**, *22*, 1353–1354.
20. Koteish, A.; Diehl, A.M. Animal models of steatosis. *Semin. Liver Dis.* **2001**, *21*, 89–104.
21. Donnelly, K.L.; Smith, C.I.; Schwarzenberg, S.J.; Jessurun, J.; Boldt, M.D.; Parks, E.J. Sources of fatty acids stored in liver and secreted via lipoproteins in patients with nonalcoholic fatty liver disease. *J. Clin. Investig.* **2005**, *115*, 1343–1351.
22. Nehra, V.; Angulo, P.; Buchman, A.L.; Lindor, K.D. Nutritional and metabolic considerations in the etiology of nonalcoholic steatohepatitis. *Dig. Dis. Sci.* **2001**, *46*, 2347–2352.
23. Bradbury, M.W. Lipid metabolism and liver inflammation. Hepatic fatty acid uptake-possible role in steatosis. *Am. J. Physiol. Gastrointest. Liver Physiol.* **2006**, *290*, 194–198.
24. Petersen, K.F.; Dufour, S.; Befroy, D.; Lehrke, M.; Hendler, R.E.; Shulman, G.I. Reversal of nonalcoholic hepatic steatosis, hepatic insulin resistance, and hyperglycemia by moderate weight reduction in patients with type 2 diabetes. *Diabetes* **2005**, *54*, 603–608.
25. Previs, S.F.; Withers, D.J.; Ren, J.M.; White, M.F.; Shulman, G.I. Contrasting effects of IRS-1 *versus* IRS-2 gene disruption on carbohydrate and lipid metabolism *in vivo* Tissue-specific insulin resistance in mice with mutations in the insulin receptor, IRS-1, and IRS-2. *J. Biol. Chem.* **2000**, *275*, 38990–38904.
26. Utzschneider, K.M.; Kahn, S.E. The role of insulin resistance in nonalcoholic fatty liver disease. *J. Clin. Endocrinol. Metab.* **2006**, *91*, 4753–4761.
27. Abdelmalek, M.F.; Diehl, A.M. Nonalcoholic fatty liver disease as a complication of insulin resistance. *Med. Clin. N. Am.* **2007**, *91*, 1125–1149.
28. Kim, J.K.; Michael, M.D.; Previs, S.F.; Peroni, O.D.; Mauvais-Jarvis, F.; Neschen, S.; Kahn, B.B.; Kahn, C.R.; Shulman, G.I. Redistribution of substrates to adipose tissue promotes obesity in mice with selective insulin resistance in muscle. *J. Clin. Investig.* **2000**, *105*, 1791–1797.
29. Koch, L.; Wunderlich, F.T.; Seibler, J.; Konner, A.C.; Hampel, B.; Irlenbusch, S.; Brabant, G.; Kahn, C.R.; Schwenk, F.; Brüning, J.C. Central insulin action regulates peripheral glucose and fat metabolism in mice. *J. Clin. Investig.* **2008**, *118*, 2132–2147.
30. Blüher, M.; Michael, M.D.; Peroni, O.D.; Ueki, K.; Carter, N.; Kahn, B.B.; Kahn, C.R. Adipose tissue selective insulin receptor knockout protects against obesity and obesity-related glucose intolerance. *Dev. Cell* **2002**, *3*, 25–38.
31. Reddy, J.K.; Rao, M.S. Lipid metabolism and liver inflammation. II. Fatty liver disease and fatty acid oxidation. *Am. J. Physiol. Gastrointest. Liver Physiol.* **2006**, *290*, 852–858.
32. Ito, M.; Suzuki, J.; Sasaki, M.; Watanabe, K.; Tsujioka, S.; Takahashi, Y.; Gomori, A.; Hirose, H.; Ishihara, A.; Iwaasa, H.; *et al.* Development of nonalcoholic steatohepatitis model through combination of high-fat diet and tetracycline with morbid obesity in mice. *Hepatol. Res.* **2006**, *34*, 92–98.

33. Ito, M.; Suzuki, J.; Tsujioka, S.; Sasaki, M.; Gomori, A.; Shirakura, T.; Hirose, H.; Ito, M.; Ishihara, A.; Iwaasa, H.; *et al.* Longitudinal analysis of murine steatohepatitis model induced by chronic exposure to high-fat diet. *Hepatol. Res.* **2007**, *37*, 50–57.

34. Deng, Q.G.; She, H.; Cheng, J.H.; French, S.W.; Koop, D.R.; Xiong, S.; Tsukamoto, H. Steatohepatitis Induced by Intragastric overfeeding in mice. *Hepatology* **2005**, *42*, 905–914.

35. Tetri, L.H.; Basaranoglu, M.; Brunt, E.M.; Yerian, L.M.; Neuschwander-Tetri, B.A. Severe NAFLD with hepatic necroinflammatory changes in mice fed trans fats and a high-fructose corn syrup equivalent. *Am. J. Physiol. Gastrointest. Liver Physiol.* **2008**, *295*, 987–995.

36. Tsuchiya, H.; Ebata, Y.; Sakabe, T. High-fat, high-fructose diet induces hepatic iron overload via a hepcidin-independent mechanism prior to the onset of liver steatosis and insulin resistance in mice. *Metabolism* **2013**, *62*, 62–69.

37. Bergheim, I.; Weber, S.; Vos, M. Antibiotics protect against fructose-induced hepatic lipid accumulation in mice: Role of endotoxin. *J. Hepatol.* **2008**, *48*, 983–992.

38. Spruss, A.; Kanuri, G.; Wagnerberger, S.; Haub, S.; Bischoff, S.C.; Bergheim, I. Toll-like receptor 4 is involved in the development of fructose-induced hepatic steatosis in mice. *Hepatology* **2009**, *50*, 1094–1104.

39. Kanuri, G.; Spruss, A.; Wagnerberger, S. Role of tumor necrosis factor alpha (TNFalpha) in the onset of fructose-induced nonalcoholic fatty liver disease in mice. *J. Nutr. Biochem.* **2011**, *22*, 527–534.

40. Tappy, L.; Le, K.A.; Tran, C. Fructose and metabolic diseases: New findings, new questions. *Nutrition* **2010**, *26*, 1044–1049.

41. Ingalls, A.M.; Dickie, M.M.; Snell, G.D. Obese, a new mutation in the house mouse. *J. Hered.* **1950**, *41*, 317–318.

42. Mayer, J.; Russell, R.E.; bates, M.W.; dickie, M.M. Metabolic, nutritional and endocrine studies of the hereditary obesity-diabetes syndrome of mice and mechanism of its development. *Metabolism* **1953**, *2*, 9–21.

43. Garthwaite, T.L.; Martinson, D.R.; Tseng, L.F.; Hagen, T.C.; Menahan, L.A. A longitudinal hormonal profile of the genetically obese mouse. *Endocrinology* **1980**, *107*, 671–676.

44. Zhang, Y.; Proenca, R.; Maffei, M.; Barone, M.; Leopold, L.; Friedman, J.M. Positional cloning of the mouse obese gene and its human homolog. *Nat. Dec.* **1994**, *372*, 425–432.

45. Pelleymounter, M.A.; Cullen, M.J.; Baker, M.B.; Hecht, R.; Winters, D.; Boone, T.; Collins, F. Effects of the obese gene product on body weight regulation in ob/ob mice. *Science* **1995**, *269*, 540–543.

46. Halaas, J.L.; Gajiwala, K.S.; Maffei, M.; Cohen, S.L.; Chait, B.T.; Rabinowitz, D.; Lallone, R.L.; Burley, S.K.; Friedman, J.M. Weight-reducing effects of the plasma protein encoded by the obese gene. *Science* **1995**, *269*, 543–546.

47. Lindström, P. The physiology of obese-Hyperglycemic mice (*ob/ob* mice). *Sci. World J.* **2007**, *29*, 666–685.

48. Hummel, K.P.; Dickie, M.M.; Coleman, D.L. Diabetes, a new mutation in the mouse. *Science* **1966**, *153*, 1127–1128.

49. Tartaglia, L.A.; Dembski, M.; Weng, X.; Deng, N.; Culpepper, J.; Devos, R.; Richards, G.J.; Campfield, L.A.; Clark, F.T.; Deeds, J. Identification and expression cloning of a leptin receptor, *OB-R. Cell* **1995**, *83*, 1263–1271.
50. Wortham, M.; He, L.; Gyamfi, M.; Copple, B.L.; Wan, Y.J. The transition from fatty liver to NASH associates with SAMe depletion in db/db mice fed a methionine choline-deficient diet. *Dig. Dis. Sci.* **2008**, *53*, 2761–2774.
51. Takaya, K.; Ogawa, Y.; Isse, N.; Okazaki, T.; Satoh, N.; Masuzaki, H.; Mori, K.; Tamura, N.; Hosoda, K.; Nakao K. Molecular cloning of rat leptin receptor isoform complementary DNAs-identification of a missense mutation in zucker fatty (*fa/fa*) rats. *Biochem. Biophys. Res. Commun.* **1996**, *225*, 75–83.
52. Balthasar, N.; Dalgaard, L.T.; Lee, C.E. Divergence of melanocortin pathways in the control of food intake and energy expenditure. *Cell* **2005**, *123*, 493–505.
53. Itoh, M.; Suganami, T.; Nakagawa, N. Melanocortin 4 receptor-deficient mice as a novel mouse model of nonalcoholic steatohepatitis. *Am. J. Pathol.* **2011**, *179*, 2454–2463.
54. Vaisse, C.; Clement, K.; Durand, E. Melanocortin-4 receptor mutations are a frequent and heterogeneous cause of morbid obesity. *J. Clin. Investig.* **2000**, *106*, 253–262.
55. Jiang, L.; You, J.; Yu, X.; Gonzalez, L.; Yu, Y.; Wang, Q.; Yang, G.; Li, W.; Li, C.; Liu, Y. Tyrosine-dependent and -independent actions of leptin receptor in control of energy balance and glucose homeostasis. *EPUB* **2008**, *105*, 18619–18624.
56. Piper, M.L.; Unger, E.K.; Myers, M.G., Jr.; Xu, A.W. Specific physiological roles for signal transducer and activator of transcription 3 in leptin receptor-expressing neurons. *Mol. Endocrinol.* **2008**, *22*, 751–759.
57. Bates, S.H.; Kulkarni, R.N.; Seifert, M.; Myers, M.G., Jr. Roles for leptin receptor/STAT3-dependent and -independent signals in the regulation of glucose homeostasis. *Cell Metab.* **2005**, *1*, 169–178.
58. Okumura, K.; Ikejima, K.; Kon, K.; Abe, W.; Yamashina, S.; Enomoto, N.; Takei, Y.; Sato, N. Exacerbation of dietary steatohepatitis and fibrosis in obese, diabetic KKAy mice. *Hepatol. Res.* **2006**, *36*, 217–228.
59. Soga, M.; Hashimoto, S.; Kishimoto, Y.; Hirasawa, T.; Makino, S.; Inagaki, S. Insulin resistance, steatohepatitis, and Hepatocellular carcinoma in a New Congenic Strain of fatty liver Shionogi (FLS) with the *Lep*^{ob} gene. *Exp. Anim.* **2010**, *59*, 407–419.
60. Kawano, K.; Hirashima, T.; Mori, S.; Saitoh, Y.; Kurosumi, M.; Natori, T. Spontaneous long-term hyperglycemic rat with diabetic complications. Otsuka Long-Evans Tokushima Fatty (OLETF) strain. *Diabetes* **1992**, *42*, 1422–1428.
61. Nielsen, S.; Guo, Z.; Johnson, C.M.; Hensrud, D.D.; Jensen, M.D. Splanchnic lipolysis in human obesity. *J. Clin. Investig.* **2004**, *113*, 1582–1588.
62. Shimomura, I.; Hammer, R.E.; Richardson, J.A.; Ikemoto, S.; Bashmakov, Y.; Goldstein, J.L.; Brown, M.S. Insulin resistance and diabetes mellitus in transgenic mice expressing nuclear SREBP-1c in adipose tissue, model for congenital generalized lipodystrophy. *Genes Dev.* **1998**, *12*, 3182–3194.

63. Moitra, J.; Mason, M.M.; Olive, M.; Krylov, D.; Gavrilova, O.; Marcus-Samuels, B.; Feigenbaum, L.; Lee, E.; Aoyama, T.; Eckhaus, M. Life without white fat, a transgenic mouse. *Genes Dev.* **1998**, *12*, 3168–3181.
64. Coburn, C.T.; Knapp, F.F., Jr.; Febbraio, M.; Beets, A.L.; Silverstein, R.L.; Abumrad, N.A. Defective uptake and utilization of long chain fatty acids in muscle and adipose tissues of CD36 knockout mice. *J. Biol. Chem.* **2000**, *275*, 32523–32529.
65. Ross, S.R.; Graves, R.A.; Spiegelman, B.M. Targeted expression of a toxin gene to adipose tissue, transgenic mice resistant to obesity. *Genes Dev.* **1993**, *7*, 1318–1324.
66. Koutnikova, H.; Cock, T.A.; Watanabe, M.; Houten. S.M.; Champy, M.F.; Dierich, A.; Auwerx, J. Compensation by the muscle limits the metabolic consequences of lipodystrophy in PPAR hypomorphic mice. *Proc. Natl. Acad. Sci. USA* **2003**, *100*, 14457–14462.
67. Tomlinson, J.W.; Walker, E.A.; Bujalska, I.J.; Draper, N.; Lavery, G.G.; Cooper, M.S.; Hewison, M.; Stewart, P.M. 11beta-hydroxysteroid dehydrogenase type 1, a tissue-specific regulator of glucocorticoid response. *Endocr. Rev.* **2004**, *25*, 831–866.
68. Morton, N.M.; Seckl, J.R. 11beta-hydroxysteroid dehydrogenase type 1 and obesity. *Front. Horm. Res.* **2008**, *36*, 146–164.
69. Laurent, V.; Kimble, A.; Peng, B.; Zhu, P.; Pintar, J.E.; Steiner, D.F.; Lindberg, I. Mortality in 7B2 null mice can be rescued by adrenalectomy, involvement of dopamine in ACTH hypersecretion. *Proc. Natl. Acad. Sci. USA* **2002**, *99*, 3087–3092.
70. Gilham, D.; Perreault, K.R.; Holmes, C.F.; Brindley, D.N.; Vance, D.E.; Lehner, R. Insulin, glucagon and fatty acid treatment of hepatocytes does not result in phosphorylation or changes in activity of triacylglycerol hydrolase. *Biochim. Biophys. Acta* **2005**, *1736*, 189–199.
71. Rossetti, L.; Barzilai, N.; Chen, W.; Harris, T.; Yang, D.; Rogler, C.E. Hepatic overexpression of insulin-like growth factor-II in adulthood increases basal and insulin-stimulated glucose disposal in conscious mice. *J. Biol. Chem.* **1996**, *271*, 203–208.
72. Zhou, Y.C.; Davey, H.W.; McLachlan, M.J.; Xie, T.; Waxman, D.J. Elevated basal expression of liver peroxisomal beta-oxidation enzymes and CYP4A microsomal fatty acid omega-hydroxylase in STAT5b$^{-/-}$ mice, cross-talk *in vivo* between peroxisome proliferator-activated receptor and signal transducer and activator of transcription signaling pathways. *Toxicol. Appl. Pharmacol.* **2002**, *182*, 1–10.
73. Browning, J.D.; Horton, J.D. Molecular mediators of hepatic steatosis and liver injury. *J. Clin. Investig.* **2004**, *114*, 147–152.
74. Foufelle, F.; Ferre, P. New perspectives in the regulation of hepatic glycolytic and lipogenic genes by insulin and glucose, a role for the transcription factor sterol regulatory element binding protein-1c. *Biochem. J.* **2002**, *366*, 377–391.
75. Trumble, G.; Smith, M.; Winder, W. Purification and characterization of rat skeletal muscle acetyl-CoA carboxylase. *Eur. J. Biochem.* **1995**, *231*, 192–198.
76. Nosadini, R.; Ursini, F.; Tessari, P.; Tiengo, A.; Gregolin, C. Perfused liver carnitine palmitoyl-transferase activity and ketogenesis in streptozotocin treated and genetic hyperinsulinemic rats. Effect of glucagon. *Horm. Metab. Res.* **1979**, *11*, 661–664.

77. Li, J.; Yen, C.; Liaw, D.; Podsypanina, K.; Bose, S.; Wang, S.I.; Puc, J.; Miliaresis, C.; Rodgers, L.; McCombie, R.; *et al.* PTEN, a putative protein tyrosine phosphatase gene mutated in human brain, breast, and prostate cancer. *Science* **1997**, *275*, 1943–1947.
78. Maehama, T.; Dixon, J.E. The tumor suppressor, PTEN/MMAC1, dephosphorylates the lipid second messenger, phosphatidylinositol 3,4,5-trisphosphate. *J. Biol. Chem.* **1998**, *273*, 13375–13378.
79. Horie, Y.; Suzuki, A.; Kataoka, E.; Sasaki, T.; Hamada, K.; Sasaki, J.; Mizuno, K.; Hasegawa, G.; Kishimoto, H.; Iizuka, M.; *et al.* Hepatocyte-specific Pten deficiency results in steatohepatitis and hepatocellular carcinomas. *J. Clin. Investig.* **2004**, *113*, 1774–1783.
80. Koh, H.J.; Lee, S.M.; Son, B.G.; Lee, S.H.; Ryoo, Z.Y.; Chang, K.T.; Park, J.-W.; Park, D.-C.; Song, B.J.; Veech, R.L.; *et al.* Cytosolic $NADP^+$-dependent isocitrate dehydrogenase plays a key role in lipid metabolism. *J. Biol. Chem.* **2004**, *279*, 39968–39974.
81. Iizuka, K.; Bruick, R.K.; Liang, G.; Horton, J.D.; Uyeda, K. Deficiency of carbohydrate response element-binding protein (ChREBP) reduces lipogenesis as well as glycolysis. *Proc. Natl. Acad. Sci. USA* **2004**, *101*, 7281–7286.
82. Takahashi, A.; Shimano, H.; Nakagawa, Y.; Yamamoto, T.; Motomura, K.; Matsuzaka, T.; Sone, H.; Suzuki, H.; Toyoshima, H.; Yamada, N.; *et al.* Transgenic mice overexpressing SREBP-1a under the control of the PEPCK promoter exhibit insulin resistance, but not diabetes. *Biochim. Biophys. Acta* **2005**, *1740*, 427–433.
83. Bennett, M.J. Pathophysiology of fatty acid oxidation disorders. *J. Inherit. Metab. Dis.* **2009**, *33*, 533–537.
84. McGarry, J.D.; Brown, N.F. The mitochondrial carnitine palmitoyltransferase system, from concept to molecular analysis. *Eur. J. Biochem.* **1997**, *244*, 1–6.
85. Yanagitani, A.; Yamada, S.; Yasui, S.; Shimomura, T.; Murai, R.; Murawaki, Y.; Hashiguchi, K.; Kanbe, T.; Saeki, T.; Ichiba, M.; *et al.* Retinoic acid receptor alpha dominant negative form causes steatohepatitis and liver tumors in transgenic mice. *Hepatology* **2004**, *40*, 366–375.
86. Fan, C.Y.; Pan, J.; Usuda, N.; Yeldandi, A.V.; Rao, M.S.; Reddy, J.K. Steatohepatitis, spontaneous peroxisome proliferation and liver tumors in mice lacking peroxisomal fatty acyl-CoA oxidase. Implications for peroxisome proliferator-activated receptor alpha natural ligand metabolism. *J. Biol. Chem.* **1998**, *273*, 15639–15645.
87. Aoyama, T.; Peters, J.M.; Iritani, N.; Nakajima, T.; Furihata, K.; Hashimoto, T.; Gonzalez, F.J. Altered constitutive expression of fatty acid-metabolizing enzymes in mice lacking the peroxisome proliferator-activated receptor alpha (PPARalpha). *J. Biol. Chem.* **1998**, *273*, 5678–5684.
88. Nemoto, Y.; Toda, K.; Ono, M.; Adachi, K.F.; Saibara, T.; Onishi, S.; Enzan, H.; Okada, T.; Shizuta, Y. Altered expression of fatty acid-metabolizing enzymes in aromatase deficient mice. *J. Clin. Investig.* **2000**, *105*, 1819–1825.
89. Kuwajima, M.; Kono, N.; Horiuchi, M.; Imamura, Y.; Ono, A.; Inui, Y.; Kawata, S.; Koizumi, T.; Hayakawa, J.; Saheki, T.; *et al.* Animal model of systemic carnitine deficiency: Analysis in C3H-H-2 degrees strain of mouse associated with juvenile visceral steatosis. *Biochem. Biophys. Res. Commun.* **1991**, *174*, 1090–1094.

90. Boison, D.; Scheurer, L.; Zumsteg, V.; Rülicke, T.; Litynski, P.; Fowler, B.; Brandner, S.; Mohler, H. Neonatal hepatic steatosis by disruption of the adenosine kinase gene. *Proc. Natl. Acad. Sci. USA* **2002**, *99*, 6985–6990.
91. Hamelet, J.; Demuth, K.; Paul, J.L.; Delabar, J.M.; Janel, N. Hyperhomocysteinemia due to cystathionine beta synthase deficiency induces dysregulation of genes involved in hepatic lipid homeostasis in mice. *Hepatology* **2007**, *46*, 151–159.
92. Arsov, T.; Larter, C.Z.; Nolan, C.J.; Petrovsky, N.; Goodnow, C.C.; Teoh, N.C.; Yeh, M.M.; Farrell, G.C. Adaptive failure to high-fat diet characterizes steatohepatitis in Alms1 mutant mice. *Biochem. Biophys. Res. Commun.* **2006**, *342*, 1152–1159.
93. Julius, U. Influence of plasma free fatty acids on lipoprotein synthesis and diabetic dyslipidemia. *Exp. Clin. Endocrinol. Diabetes* **2003**, *111*, 246–250.
94. Gordon, D.A. Recent advances in elucidating the role of the microsomal triglyceride transfer protein in apolipoprotein B lipoprotein assembly. *Curr. Opin. Lipidol.* **1997**, *8*, 131–137.
95. Wetterau, J.R.; Gregg, R.E.; Harrity, T.W.; Arbeeny, C.; Cap, M.; Connolly, F.; Chu, C.H.; George, R.J.; Gordon, D.A.; Jamil, H.; *et al.* An MTP inhibitor that normalizes atherogenic lipoprotein levels in WHHL rabbits. *Science* **1998**, *282*, 751–754.
96. Rinella, M.E.; Elias, M.S.; Smolak, R.R.; Fu, T.; Borensztajn, J.; Green, R.M. Mechanisms of hepatic steatosis in mice fed a lipogenic methionine choline-deficient diet. *J. Lipid Res.* **2008**, *49*, 1068–1076.
97. Raabe, M.; Véniant, M.M.; Sullivan, M.A.; Zlot, C.H.; Björkegren, J.; Nielsen, L.B.; Wong, J.S.; Hamilton, R.L.; Young, S.G. Analysis of the role of microsomal triglyceride transfer protein in the liver of tissue-specific knockout mice. *J. Clin. Investig.* **1999**, *103*, 1287–1298.
98. Helmkamp, G.M., Jr.; Harvey, M.S.; Wirtz, K.W.; Van Deenen, L.L. Phospholipid exchange between membranes. Purification of bovine brain proteins that preferentially catalyze the tranfer of phosphatidylinositol. *J. Biol. Chem.* **1974**, *249*, 6382–6389.
99. Alb, J.G., Jr.; Cortese, J.D.; Phillips, S.E.; Albin, R.L.; Nagy, T.R.; Hamilton, B.A.; Bankaitis V.A. Mice lacking phosphatidylinositol transfer protein-alpha exhibit spinocerebellar degeneration, intestinal and hepatic steatosis, and hypoglycemia. *J. Biol. Chem.* **2003**, *278*, 33501–33518.
100. Zhu, X.; Song, J.; Mar, M.H.; Edwards, L.J.; Zeisel, S.H. Phosphatidylethanolamine *N*-methyltransferase (PEMT) knockout mice have hepatic steatosis and abnormal hepatic choline metabolite concentrations despite ingesting a recommended dietary intake of choline. *Biochem. J.* **2003**, *370*, 987–993.
101. Hussain, M.M.; Maxfield, F.R.; Más-Oliva, J.; Tabas, I.; Ji, Z.S.; Innerarity, T.L.; Mahley, R.W. Clearance of chylomicron remnants by the low density ipoprotein receptor-related protein/alpha 2-macroglobulin receptor. *J. Biol. Chem.* **1991**, *266*, 13936–13940.
102. Ma, K.L.; Ruan, X.Z.; Powis, S.H.; Chen, Y.; Moorhead, J.F.; Varghese, Z. Inflammatory stress exacerbates lipid accumulation in hepatic cells and fatty livers of apolipoprotein E knockout mice. *Hepatology* **2008**, *48*, 770–781.
103. Vlahcevic, Z.R.; Stravitz, R.T.; Heuman, D.M.; Hylemon, P.B.; Pandak, W.M. Quantitative estimations of the contribution of different bile acid pathways to total bile acid synthesis in the rat. *Gastroenterology* **1997**, *113*, 1949–1957.

104. Feng, B.; Yao, P.M.; Li, Y.; Devlin, C.M.; Zhang, D.; Harding, H.P.; Sweeney, M.; Rong, J.X.; Kuriakose, G.; Fisher, E.A.; *et al.* The endoplasmic reticulum is the site of cholesterol-induced cytotoxicity in macrophages. *Nat. Cell Biol.* **2003**, *5*, 781–792.
105. Devries-Seimon, T.; Li, Y.; Yao, P.M.; Stone, E.; Wang, Y.; Davis, R.J.; Flavell, R.; Tabas, I. Cholesterol-induced macrophage apoptosis requires ER stress pathways and engagement of the type A scavenger receptor. *J. Cell. Biol.* **2005**, *171*, 61–73.
106. Bieghs, V.; Verheyen, F.; van, Gorp, P.J.; Hendrikx, T.; Wouters, K.; Lütjohann, D.; Gijbels, M.J.; Febbraio, M.; Binder, C.J.; Hofker, M.H.; *et al.* Internalization of modified lipids by CD36 and SR-A leads to hepatic inflammation and lysosomal cholesterol storage in Kupffer cells. *PLoS One* **2012**, *7*, e34378.
107. Puri, P.; Baillie, R.A.; Wiest, M.M.; Mirshahi, F.; Choudhury, J.; Cheung, O.; Sargeant, C.; Contos, M.J.; Sanyal, A.J. A lipidomic analysis of nonalcoholic fatty liver disease. *Hepatology* **2007**, *46*, 1081–1090.
108. Isoda, K.; Sawada, S.; Ayaori, M.; Matsuki, T.; Horai, R.; Kagata, Y.; Miyazaki, K.; Kusuhara, M.; Okazaki, M.; Matsubara, O. Deficiency of interleukin-1 receptor antagonist deteriorates fatty liver and cholesterol metabolism in hypercholesterolemic mice. *J. Biol. Chem.* **2005**, *280*, 7002–7009.
109. Otogawa, K.; Kawada, N. A rabbit model for the study of human NASH. *Nippon Rinsho* **2006**, *64*, 1043–1047.
110. Matteoni, C.A.; Younossi, Z.M.; Gramlich, T.; Boparai, N.; Liu, Y.C.; McCullough, A.J. Nonalcoholic fatty liver disease: A spectrum of clinical and pathological severity. *Gastroenterology* **1999**, *116*, 1413–1419.
111. Brunt, E.M.; Neuschwander-Tetri, B.A.; Oliver, D.; Wehmeier, K.R.; Bacon, B.R. Nonalcoholic steatohepatitis: Histologic features and clinical correlations with 30 blinded biopsy specimens. *Hum. Pathol.* **2004**, *35*, 1070–1082.
112. Burt, A.D.; Mutton, A.; Day, C.P. Diagnosis, interpretation of steatosis and steatohepatitis. *Semin. Diagn. Pathol.* **1998**, *15*, 246–258.
113. Yahagi, N.; Shimano, H.; Matsuzaka, T.; Sekiya, M.; Najima, Y.; Okazaki, S.; Okazaki, H.; Tamura, Y.; Iizuka, Y.; Inoue, N. p53 Involvement in the Pathogenesis of Fatty Liver Disease. *J. Biol. Chem.* **2004**, *279*, 20571–20575.
114. Xu, H.; Barnes, G.T.; Yang, Q.; Tan, G.; Yang, D.; Chou, C.J.; Sole, J.; Nichols, A.; Ross, J.S.; Tartaglia, L.A.; *et al.* Chronic inflammation in fat plays a crucial role in the development of obesity-related insulin resistance. *J. Clin. Investig.* **2003**, *112*, 1821–1830.
115. Imajo, K.; Fujita, K.; Yoneda, M.; Nozaki, Y.; Ogawa, Y.; Shinohara, Y.; Kato, S.; Mawatari, H.; Shibata, W.; Kitani, H.; *et al.* Hyperresponsivity to low-dose endotoxin during progression to nonalcoholic steatohepatitis is regulated by leptin-mediated signaling. *Cell Metab.* **2012**, *16*, 44–54.

Carcinogenesis vol.35 no.2 pp.272–281, 2014
doi:10.1093/carcin/bgt343
Advance Access publication October 15, 2013

Heat shock factor 1 accelerates hepatocellular carcinoma development by activating nuclear factor-κB/mitogen-activated protein kinase

Makoto Chuma*, Naoya Sakamoto, Akira Nakai[1], Shuhei Hige, Mitsuru Nakanishi, Mitsuteru Natsuizaka, Goki Suda, Takuya Sho, Kanako Hatanaka[2], Yoshihiro Matsuno[2], Hideki Yokoo[3], Toshiya Kamiyama[3], Akinobu Taketomi[3], Gen Fujii[4], Kosuke Tashiro[5], Yoko Hikiba[6], Mitsuaki Fujimoto[1], Masahiro Asaka and Shin Maeda[7]

Department of Gastroenterology and Hepatology, Hokkaido University, Kita 15, Nishi 7, Kita-ku, Sapporo 060-8638, Japan, [1]Department of Biochemistry and Molecular Biology, Yamaguchi University, Ube, Japan, [2]Department of Pathology and [3]Department of Gastroenterological Surgery I, Hokkaido University, Kita 15, Nishi 7, Kita-ku, Sapporo 060-8638, Japan, [4]Division of Cancer Prevention, National Cancer Center Research Institute, Tokyo, Japan, [5]Graduate School of Genetic Resources Technology, Kyushu University, Fukuoka, Japan, [6]Division of Gastroenterology, Institute for Adult Diseases, Asahi Life Foundation, Tokyo, Japan and [7]Department of Gastroenterology, Yokohama City University, Yokohama, Japan

*To whom correspondence should be addressed. Tel: +81 11-716-1611; Fax: +81 11-706-7867;
Email: mchuuma@med.hokudai.ac.jp

Heat shock factor 1 (HSF1), a major transactivator of stress responses, has been implicated in carcinogenesis in various organs. However, little is known about the biological functions of HSF1 in the development of hepatocellular carcinoma (HCC). To clarify the functional role of HSF1 in HCC, we established HSF1-knockdown (HSF1 KD) KYN2 HCC cells by stably expressing either small hairpin RNA (shRNA) against HSF1 (i.e. HSF1 KD) or control shRNA (HSF1 control). Tumorigenicity was significantly reduced in orthotopic mice with HSF1 KD cells compared with those with HSF1 control cells. Reduced tumorigenesis in HSF1 KD cells appeared attributable to increased apoptosis and decreased proliferation. Tumor necrosis factor-α-induced apoptosis was increased in HSF1 KD cells and HSF1$^{-/-}$ mouse hepatocytes compared with controls. Decreased expression of IκB kinase γ, a positive regulator of nuclear factor-κB, was also observed in HSF1 KD cells and HSF1$^{-/-}$ mouse hepatocytes. Furthermore, expression of bcl-2-associated athanogene domain 3 (BAG3) was dramatically reduced in HSF1 KD cells and HSF1$^{-/-}$ mouse hepatocytes. We also found that epidermal growth factor-stimulated mitogen-activated protein kinase signaling was impaired in HSF1 KD cells. Clinicopathological analysis demonstrated frequent overexpression of HSF1 in human HCCs. Significant correlations between HSF1 and BAG3 protein levels and prognosis were also observed. In summary, these results identify a mechanistic link between HSF1 and liver tumorigenesis and may provide as a potential molecular target for the development of anti-HCC therapies.

Introduction

Hepatocellular carcinoma (HCC) is one of the most common malignant tumors and the third leading cause of cancer death worldwide (1). Despite marked advances in diagnostic and therapeutic techniques, prognosis remains unsatisfactory for HCC patients (2,3). An understanding of HCC carcinogenesis at the molecular level is thus urgently needed in order to identify novel molecular targets for the development of more effective therapies.

Heat shock factor 1 (HSF1) is the main regulator of the heat shock response, which is involved in protecting cells and organisms from heat, ischemia, inflammation, oxidative stress and other noxious conditions (4,5). Under various forms of physiological stress, HSF1 drives the production of heat shock proteins (HSPs), such as HSP27, HSP70 and HSP90, which act as protein chaperones (5,6). The functions of HSF1 are not limited to increasing the expression of chaperones; HSF1 also modulates the expression of hundreds of genes other than chaperones that are critical for survival under an array of potentially lethal stressors (6–8). As a result, HSF1 influences fundamental cellular processes such as cell cycle control, protein translation, glucose metabolism and proliferation (7–12). In human tumors, constitutive expression of Hsp27, Hsp70 and Hsp90 at high levels predicts poor prognosis and resistance to therapy (13–15). These effects are often attributable to HSF1-dependent mechanisms (16). Thus, as a master regulator of cellular processes, the roles of HSF1 in carcinogenesis and tumor progression are now emerging. Several recent investigations using mouse models have suggested that HSF1 is involved in carcinogenesis (9,17). In clinical samples, HSF1 is often constitutively expressed at high levels in a variety of tumors, including breast cancer (7,18), pancreatic cancer (19), prostate carcinoma (20) and oral squamous cell carcinoma (21).

Hepatocarcinogenesis is a multistep process, in the majority of cases slowly developing within a well-defined etiology of viral infection and chronic alcohol abuse, leading to the chronic hepatitis and cirrhosis that are regarded as preneoplastic stages (22). A great number of factors, receptors and downstream elements of signaling cascades regulate proliferation and apoptosis. Dysregulation of the balance between cell proliferation and apoptosis thus plays a critical role in hepatocarcinogenesis (23,24). Two of the major pathways of cell proliferation and apoptosis are nuclear factor kappa B (NF-κB) signaling and mitogen-activated protein kinase (MAPK) signaling. NF-κB transcription factors are critical regulators of genes involved in inflammation and the suppression of apoptosis. NF-κB has been shown to be instrumental for tumor promotion in colitis-associated cancer and inflammation-associated liver cancer (25,26). Activation of the extracellular signal-regulated kinase (ERK)/MAPK pathway regulates many important cellular processes, such as proliferation, differentiation, angiogenesis, survival and cell adhesion (27). Importantly, the ERK/MAPK pathway is constitutively activated in HCC (28).

The present study investigated the biological influences of HSF1 in HCC cell proliferation and apoptosis involving the NF-κB and MAPK signal pathways. We found that HSF1 deficiency significantly diminished NF-κB and MAPK activation in primary hepatocytes and HCC cells, so HSF1 deficiency inhibited the development of HCC. Furthermore, clinicopathological analysis demonstrated a significant correlation between HSF1 protein level and prognosis. Our results suggest HSF1 as a promising molecular target for the development of anti-HCC therapeutics.

Abbreviations: BAG3, bcl-2-associated athanogene domain 3; EGFR, epidermal growth factor receptor; ERK, extracellular signal-regulated kinase; FACS, fluorescence-activated cell sorting; HCC, hepatocellular carcinoma; HSF1, heat shock factor 1; HSF1 KD, HSF1 knockdown; HSP, heat shock protein; IKKγ, IκB kinase gamma; LPS, lipopolysaccharide; MAPK, mitogen-activated protein kinase; MEK, mitogen-activated protein kinase kinase; mRNA, messenger RNA; NF-κB, nuclear factor kappa B; PCNA, proliferating cell nuclear antigen; SCID, severe combined immune-deficient mice; shRNA, small hairpin RNA; TNF-α, tumor necrosis factor alpha; TUNEL, terminal deoxynucleotidyl transferase-mediated deoxyuridine triphosphate nick-end labeling; WT, wild type.

Materials and methods

Cell cultures and reagents

Human HCC cell lines HepG2, PLC/PRF/5, HLE and HLF were obtained from the American Type Culture Collection. Huh7 was obtained from the Japanese Collection of Research Bioresources Cell Bank (Ibaraki, Japan). KIM-1 and KYN2 were kindly provided by Dr Hirohisa Yano (Department of Pathology, Kurume University, Kurume, Japan). Li7 was kindly provided by Dr Yae Kanai (Division of Molecular Pathology, National Cancer Center Research Institute,

Tokyo, Japan). HepG2, PLC/PRF/5, Huh7, HLE and HLF cells were maintained in Dulbecco's modified Eagle's medium containing 10% fetal bovine serum. KIM-1 and KYN2 was maintained in RPMI medium containing 10% fetal bovine serum.

Antibodies and chemicals

The antibodies used included: anti-HSF1, ERK1/2, phosphor-ERK1/2, MAPK kinase (MEK), phospho-MEK, phosphor- efficiently activated epidermal growth factor receptor (EGFR), cyclin D1, cdc2, CDK4, phospho-IκBα, IκB kinase gamma (IKKγ), IKKβ, caspase-3 and Bcl-X_L (Cell Signaling Biotechnology, Danvers, MA); anti-HSP90, HSP72, β-actin and proliferating cell nuclear antigen (PCNA) (Santa Cruz Biotechnology, Santa Cruz, CA); anti-EGFR (Millipore, Billerica, MA); anti-HSP70/HSP72 (Enzo Life science, NY); and anti-BAG3 (Abcam, Cambridge, UK).

Biochemical and immunohistochemical analyses

Protein lysates were prepared from tissues and cultured cells, separated by sodium dodecyl sulfate–polyacrylamide gel electrophoresis, transferred onto Immobilon membranes (Millipore) and analyzed by immunoblotting. Total cellular RNA was extracted using Trizol reagent (Invitrogen, Carlsbad, CA), then cDNA was synthesized using SuperScript II (Invitrogen), and expression of specific messenger RNAs (mRNAs) was quantified using real-time PCR and normalized against glyceraldehyde-3-phosphate dehydrogenase mRNA expression. Details of real-time PCR conditions and primer sequences are available in Supplementary Materials and methods, available at *Carcinogenesis* Online. Immunohistochemical staining was performed on formalin-fixed, paraffin-embedded tissue sections using immunoperoxidase methods, as described previously (15). For array analysis, we used the Human WG-6 BeadChip-kit (Illumina, San Diego, CA) in accordance with the instructions from the manufacturer (details are given in Supplementary Materials and methods, available at *Carcinogenesis* Online).

Establishment of HSF1-knockdown cells

A HSF1 small hairpin RNA (shRNA) plasmid and negative control plasmid were purchased from SABiosciences (QIAGEN, Valencia, CA). The shRNA sequences targeting HSF1 were from position 5′-CAGGTTGTTCATAGTCAGAAT-3′ as in the nucleotide sequence of HSF1. As a negative control, a shRNA was designed with the sequence 5′-GGAATCTCATTCGATGCATAC-3′. Transfection was achieved using Oligofectamine reagent (Invitrogen) according to the instructions from the manufacturer. To establish stable knockdown cell lines, shRNA plasmids were transfected into KYN2 cells and cultured in the presence of puromycin (Sigma–Aldrich, St Louis, MO).

Cell proliferation and bromodeoxyuridine assay

Cell proliferation in response to HSF1 silencing was determined by trypan blue exclusion assay. DNA synthesis was determined by bromodeoxyuridine assay according to the instructions from the manufacturer (Roche Diagnostics, Basel, Switzerland). The result was expressed as a percentage of the maximum absorbance at 450 nm, based on three independent experiments. Cells were counted using a Coulter Counter (Beckman Coulter, Pasadena, CA).

Apoptosis assay

Assessment of apoptosis was performed by measuring the intensity of the sub-G_1 peak. For the sub-G_1 peak, HSF1 control KYN2 cells or HSF1-knockdown (HSF1 KD) KYN2 cells were tumor necrosis factor alpha (TNF-α) treatment for 24 h. Cells were treated with propidium iodide and then the sub-G_1 peak was analyzed with a fluorescence-activated cell sorting (FACS) flow cytometer (FACSCalibur; Becton Dickinson, San Jose, CA). Terminal deoxynucleotidyl transferase-mediated deoxyuridine triphosphate nick-end labeling (TUNEL) assay was performed in accordance with the manufacturer's instructions (ApopTag kit; Intergen, Burlington, MA).

Animals

HSF1-deficient ($HSF^{-/-}$) mice have been described previously (29). C57BL/6 wild-type (WT) mice were purchased from CLEA Japan (Tokyo, Japan) for use in the experiments, with primary hepatocytes isolated using a collagenase perfusion method as described in a previous report (26). For orthotopic implantation, C.B-17/Icr-scid/scidJcl [severe combined immune-deficient mice (SCID)] mice were obtained from CLEA Japan. All mice were maintained in filter-topped cages on autoclaved food and water at the University of Hokkaido and the Institute for Adult Diseases, Asahi Life Foundation, according to National Institutes of Health (NIH) guidelines. All experimental protocols were approved by the ethics committee for animal experimentation at Hokkaido University and Asahi Life Foundation. Orthotopic implantation of KYN2 cells and KYN2 transfectants were performed as described previously (30). Briefly, mice were inoculated orthotopically with 5×10^6 HSF1 control ($n = 12$) and HSF1 KD ($n = 12$) cells in 100 μl of phosphate-buffered saline, injected into the liver. Mice were killed 6 weeks after inoculation and autopsies were performed immediately. In the lipopolysaccharide (LPS)/D-galactosamine (GalN)-induced liver injury model, mice were injected intraperitoneally with LPS (20 lg/kg; Sigma) and GalN (1000 mg/kg; Wako, Osaka, Japan) (24).

Patients and tissue samples

For immunohistochemical analysis, a total of 226 adult patients with HCC who underwent curative resection between 1997 and 2006 at Hokkaido University Hospital were enrolled in this study. A preoperative clinical diagnosis of HCC was required to meet the diagnostic criteria of the American Association for the Study of Liver Diseases. Briefly, inclusion criteria were as follows: (i) distinctive pathological diagnosis, (ii) no preoperative anticancer treatment or distant metastases, (iii) curative liver resection (exclusion of extrahepatic tumor spread/metastasis) and (iv) complete clinicopathological and follow-up data. The study protocols were approved by the institutional review board and performed in compliance with the Helsinki of Declaration. Written informed consent was obtained from as many of the patients who were alive as possible (deceased cases were approved for use without written informed consent). Histological diagnosis was made according to World Health Organization criteria. The main clinicopathological features are presented in Table 1. During follow-up, clinical evaluations and biochemical tests were performed every 1–3 months. Patients underwent triphasic computed tomography of the liver every 2–3 months.

Statistical analysis

Data are expressed as mean ± standard error of the mean (SEM). Significant differences were detected using non-parametric testing. Correlations between protein expression and clinicopathological features of the specimens were assessed, and the resulting data were analyzed using the χ^2 test and Fisher's exact test. Cumulative survival rate was calculated from the first date of treatment using the Kaplan–Meier life-table method. Differences were evaluated by log-rank testing. Independent factors for survival were assessed with the Cox proportional hazard regression model. Differences between the two groups were analyzed using the log-rank test. Statistical analyses were performed using Stat View software (version 5.0; SAS Institute, Cary, NC). Values of $P < 0.05$ were considered significant.

Results

Effect of HSF1 on tumor growth

We first investigated expression of HSF1 in cultured HCC cell lines. HSF1 expression was detected in all eight HCC cell lines analyzed. KYN2 cells showed significantly higher expression of HSF1 than other cell lines (Figure 1A). To further elucidate the functional role of HSF1 in HCC, we established HSF1 KD KYN2 cells by expressing the shRNA against HSF1 or control shRNA. To evaluate the effects of HSF1 on cell growth, we measured cell numbers at several time points and found that the growth of HSF1 KD cells was significantly inhibited compared with control cells (HSF1 control) (Figure 1B). Cell cycle regulators including PCNA, cyclin D1, cdc2 and CDK4 were suppressed in HSF1 KD cells compared with HSF1 control cells (Figure 1C). These results indicate that HSF1 enhances HCC cell growth. Concordantly, HSF1 KD reduced DNA synthesis as measured by bromodeoxyuridine incorporation (Figure 1D).

To evaluate the effects of HSF1 on HCC *in vivo*, orthotopic xenografts were established by HSF1 control and HSF1 KD KYN2 cells in nude mice. Maximum primary tumor diameters and tumor volumes were significantly decreased in HSF1 KD xenografts compared with HSF1 control ones (Figure 1E), suggesting that HSF1 accelerated HCC tumor growth *in vivo*. We confirmed that the tumor of HSF1 KD cells showed significantly lower expression of HSF1 and PCNA than the tumor of HSF1 control cells (Figure 1E).

We performed gain-of-function experiments for HSF1 *in vitro*. No apparent changes in cell growth were seen with overexpression of HSF1 in HCC cell lines with low HSF1 expression (Supplementary Figure 1, available at *Carcinogenesis* Online), whereas cell growth was reduced in HSF1 KD experiments, as above. Based on these

Table I. HSF1, BAG3 expression and clinicopathological variables in HCC

Parameter	Total	HSF1		*P*	BAG3		*P*
		High	Low		High	Low	
		n = 115	*n* = 111		*n* = 112	*n* = 114	
		≥30	<30		≥25	<25	
Age (years)							
≥60	126	66	60	0.69	59	67	0.42
<60	100	49	51		53	47	
Sex							
Male	185	95	90	0.86	94	91	0.49
Female	41	20	21		18	23	
Etiology							
HBsAg(+)/HCV(−)	85	45	40	0.70	39	46	0.67
HBsAg(−)/HCV(+)	84	43	41		44	40	
HBsAg(+)/HCV(+)	6	4	2		2	4	
HBsAg(−)/HCV(−)	51	23	28		27	24	
Cirrhosis							
Presence	121	64	57	0.59	62	59	0.59
Absence	105	51	54		50	55	
Tumor size (cm)							
<5	149	67	82	0.017*	66	83	0.035*
≥5	77	48	29		46	31	
No. of tumor nodules							
Solitary	168	78	90	0.032*	79	89	0.22
Multiple (≥2)	58	37	21		33	25	
TNM stage							
I and II	139	62	77	0.017*	63	76	0.11
III and IV	87	53	34		49	38	
BCLC stage							
A	81	27	54	<0.001*	32	49	0.065
B	108	64	44		58	50	
C	37	24	13		22	15	
Differentiation							
Well	36	11	25	0.010*	10	26	0.014*
Moderate	143	74	69		75	68	
Poor	47	30	17		27	20	
Capsular formation							
Presence	184	95	89	0.73	91	93	1.0
Absence	42	20	22		21	21	
Vascular invasion							
Present	37	24	13	0.073	22	15	0.21
Absent	189	91	98		90	99	
Serum AFP level							
<20	117	53	64	0.086	52	65	0.14
≥20	109	62	47		60	49	

AFP, alpha-fetoprotein; BCLC, Barcelona Clinic Liver Cancer; HCV, hepatitis C virus; TNM, tumor node metastasis.
*Significant *P* value.

findings, we concluded that HSF1 expression is a necessary condition for cell growth, but it is not a sufficient condition. We, therefore, did not further investigate gain of function of HSF1.

Impaired EGF-mediated MEK/ERK activation in HSF1 KD cells and HSF1$^{-/-}$ hepatocytes

Activation of the MEK/ERK pathway regulates many important cellular processes in carcinogenesis. To further elucidate the function of HSF1 on tumor growth, we investigated the cascade of MAPK. In WT hepatocytes and HSF1 control cells, EGF, a potent activator of MAPK, efficiently activated EGFR, MEK1/2 and ERK1/2 (Figure 2A). In contrast, activation of EGFR, MEK1/2 or ERK1/2 was significantly decreased in HSF-knockout mice (HSF$^{-/-}$) hepatocytes and HSF1 KD cells (Figure 2A and B). Regarding protein levels of EGFR, MEK1/2 and ERK1/2, EGFR protein levels were significantly decreased in HSF1$^{-/-}$ hepatocytes and HSF1 KD compared with controls, whereas other proteins were unchanged (Figure 2A and B). This result was consistent with the previous report (31). Immunohistochemical staining revealed that HSF1 control tumor showed strong phosphorylated ERK1/2 levels, whereas almost no ERK1/2 activation was observed in HSF1 KD tumors (Figure 2C).

Role of HSF1 in TNF-α-induced apoptosis

Since tumor growth inhibition is caused mainly by increased cell death and decreased cellular proliferation, we compared numbers of apoptotic cell deaths in HSF1 control and HSF KD xenografts using the TUNEL assay. Significantly more apoptotic tumor cells were found in HSF1 KD tumors than in HSF1 control tumors (Figure 3A). Next, we examined whether HSF1 was involved in apoptosis *in vitro*. FACS analysis showed very few apoptotic cells in HSF KD or HSF control in the absence of any stimuli. In contrast, treatment with TNF-α, a potent inducer of apoptosis, caused more extensive apoptotic cell death in HSF1 KD cells (23.9%) than in HSF control cells (8.7%) (Figure 3B). Furthermore, we also confirmed increased TNF-α-induced apoptosis in HSF KD cells as determined by TUNEL assay and caspase-3 activation (Figure 3C and D). To examine whether HSF1 is required for TNF-α-induced liver apoptosis *in vivo*, we used an LPS/GalN liver injury model that depends on TNF-α-mediated apoptosis (32). At 7 h LPS/GalN

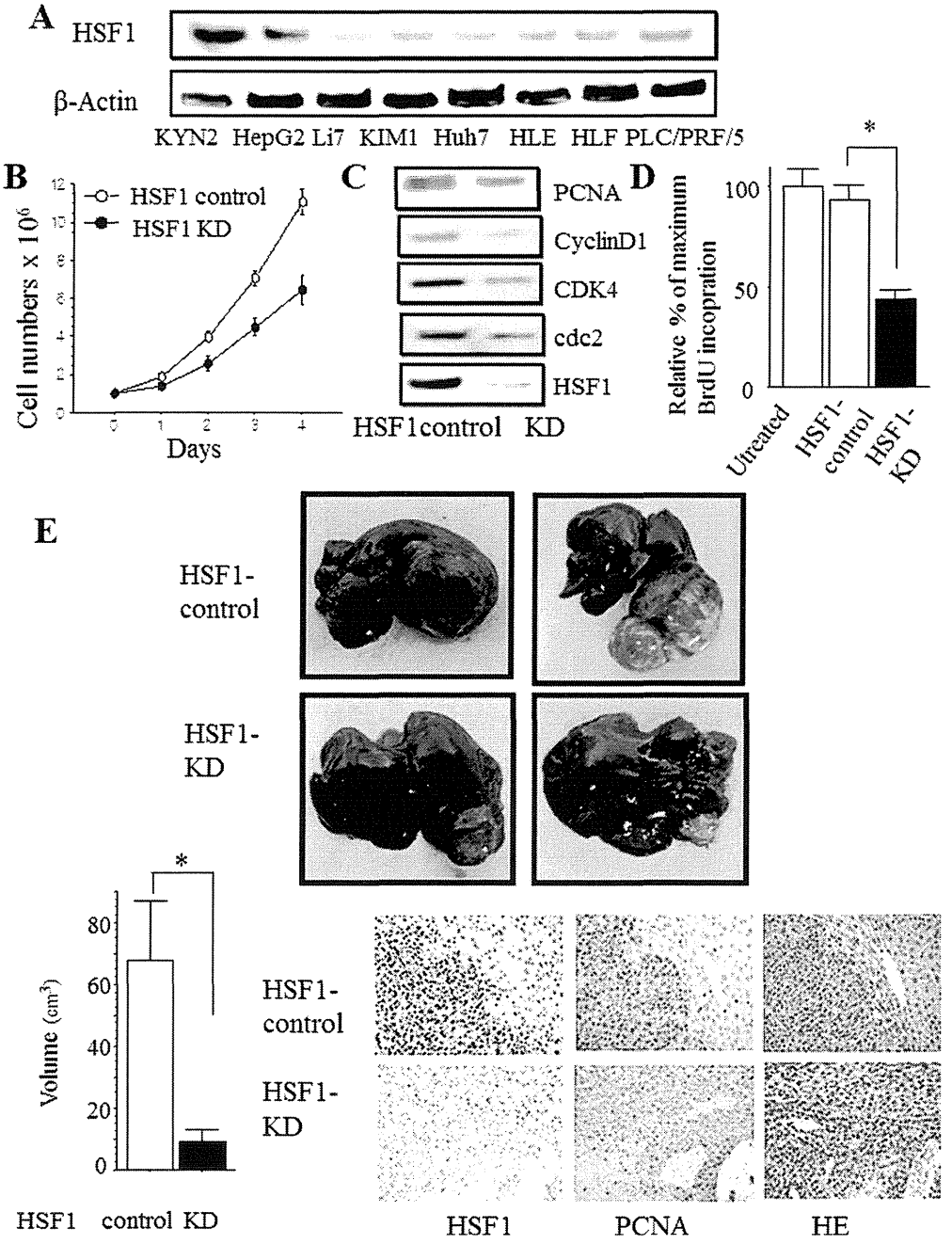

Fig. 1. Role of HSF1 in HCC growth. (**A**) Expression of HSF1 in the eight indicated HCC cell lines was determined by western blot analysis, using β-actin as a control. (**B**) Cell growth of HSF1 control KYN2 cells and HSF1 KD KYN2 cells was measured by counting the number of cells. One representative experiment from three experiments is shown. Data are plotted as mean ± SEM. (**C**) Expression of cell-cycle-related protein in HSF1 control KYN2 cells and HSF1 KD KYN2 cells, as determined by western blot analysis. (**D**) Cells were pulsed with BrdU (10 mmol/l) for 4 h. Optical density values are expressed as a percentage relative to the group expressing control. $^*P < 0.05$. Bars: SEM. (**E**) Growth appearance of HSF1 KD and HSF1 control cells in SCID mice after orthotopic implantation (upper panel). Orthotopic tumor volume was measured. Data are expressed as mean ± SEM (HSF1 control, $n = 12$; HSF1 KD, $n = 12$). $^*P < 0.05$. Bars: SEM (lower left panel). HE and immunohistochemical staining for HSF1 and PCNA (original magnification: ×40): lower right panel. BrdU, bromodeoxyuridine; HE, hematoxylin and eosin.

administration, $HSF^{-/-}$ exhibited marked alanine aminotransferase elevation (Figure 3E), severe histological liver damage and hepatocyte apoptosis compared with WT mice (Figure 3E). This was also in accordance with the notable depression of HSF1 inducing apoptosis *in vitro*.

HSF1 is involved in TNF-α-mediated NF-κB activation

Regarding the association between HSF1 and antiapoptosis, expression of bcl-2-associated athanogene domain 3 (BAG3) was reportedly reduced in HSF1 KD cells compared with control cells (7,11). In addition, microarray array analysis showed that BAG3 was dramatically downregulated in HSF1 KD cells compared with HSF1 control cells (Supplementary Table I, available at *Carcinogenesis* Online). Immunoblot analysis showed that BAG3 protein expression was reduced in $HSF1^{-/-}$ hepatocytes and HSF1 KD cells relative to the respective controls (Figure 4A and B). Meanwhile, activation of IKK and NF-κB pathway represents one of the most important antiapoptotic signals. In addition, BAG3 is also reported to control proteasomal degradation of IKKγ, the regulatory subunit (also called NF-κB essential modulator) of the IKK complex, and

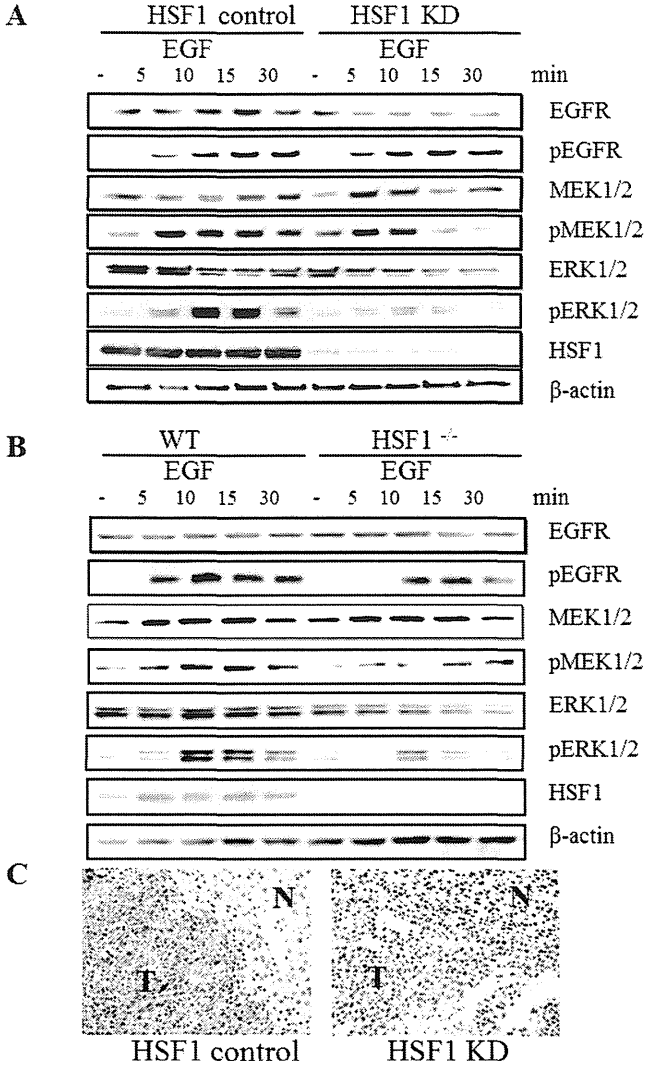

Fig. 2. EGF-mediated MEK/ERK activation is impaired in HSF1 KD cells and HSF1$^{-/-}$ hepatocytes. (**A**) HSF1 control and KD cells were treated with EGF (10 ng/ml), lysed at the indicated times, gel separated and immunoblotted with antibodies against indicated proteins. (**B**) HSF1 WT and HSF$^{-/-}$ hepatocytes were treated with TNF-α (30 ng/ml), lysed in indicated times, gel separated and immunoblotted with antibodies against indicated proteins. (**C**) Representative phosphorylated ERK (p-ERK) staining of orthotopic tumors of HSF1 control and KD cells (original magnification: ×40). N, non-cancerous liver; T, tumor.

NF-κB activity (33). Regarding the NF-κB pathway, NF-κB activation by TNF-α was decreased in HSF1 KD cells compared with the control cells (Figure 4A). In contrast, without any treatment, basal NF-κB activity was very weak and no differences were apparent between HSF1 control cells and HSF1 KD cells (Figure 4A). Consistent with this, microarray analysis showed no apparent differences in the expression of typical NF-κB-regulated genes. We also performed NF-κB pathway analysis and found that the pathway was not overrepresented by the microarray results (Supplementary Figure 2, available at *Carcinogenesis* Online). Next, we investigated whether HSF1 is involved in TNF-α-mediated NF-κB activation and found that phosphorylated Iκk-B (p-IκB), a marker of NF-κB activation, was significantly decreased in HSF$^{-/-}$ hepatocytes and HSF1 KD cells compared with their controls. As expected, IKKγ protein levels were dramatically reduced in HSF1$^{-/-}$ hepatocytes and HSF1 KD cells compared with their controls (Figure 4A and B). To investigate whether decreased IKKγ protein was degraded via proteasome, we used the proteasomal inhibitor, MG-132, and found that protein levels of IKKγ in HSF1 KD cells recovered with the inhibitor, whereas protein expression of BAG3 was unchanged (Figure 4C). Although mRNA levels of BAG3 were significantly downregulated in HSF1 KD cells compared with HSF1 control cells, mRNA levels of IKKγ were not changed (Figure 4D). HSP70 mRNA and protein levels were similar between HSF1 control and HSF1 KD cells (Figure 4A–D). These results suggest that HSF1 positively regulated BAG3 expression, which stabilized the IKKγ protein necessary for NF-κB activation. Immunohistochemical staining revealed that downregulation of HSF1 dramatically reduced BAG3 levels in HSF1 KD xenografts compared with the HSF1 control xenografts.

We performed real-time PCR analysis of the putative NF-κB-regulated antiapoptotic genes. The levels of A20, cellular inhibitor of apoptosis 2 (c-IAP2) RNA expression were decreased in HSF1 KD cells by TNF-α-mediated compared with HSF1 control cells, whereas cylindromatosis, cIAP1 were unchanged (Figure 4E). These results suggest that HSF1 plays an important role in tumor growth via MAPK-mediated cellular proliferation and NF-κB-mediated antiapoptosis.

HSF1 and BAG3 were frequently overexpressed in human HCCs

To analyze the involvement of HSF1 in HCCs, we examined expression levels of HSF1 in human primary HCCs. Immunoblot analysis showed that levels of HSF1 in HCC tissues were significantly higher than in non-cancerous liver tissues in 5 of 10 samples (50%) (Figure 5A). We tested 226 samples from tumor tissues of patients with HCCs by immunohistochemistry. The median percentage of positive cells was 30% (range: 0–90.0%) and we divided patients into two groups of high expressers and low expressers based on the percentage of HSF1-positive cells using a cutoff level of 30%, representing the median value of HSF1. We found that 50.9% (115/226) of tumor samples showed high HSF1 expression. Typical examples of high HSF1 expression samples are shown in Figure 5B. The characteristics of patients in this analysis are shown in Table I. Significant differences were apparent between high and low HSF1 expression groups in terms of tumor size ($P = 0.017$), tumor node metastasis stage ($P = 0.017$), Barcelona Clinic Liver Cancer stage ($P < 0.001$), number of tumor nodules ($P = 0.032$) and histological grade ($P = 0.010$) (Table I), but no significant correlations were observed between HSF1 expression and other clinicopathological variables such as etiology or cirrhosis (Table I). Furthermore, patients with tumors showing HSF1 overexpression displayed significantly shorter overall survival (median: 75.2 months) compared with patients whose tumors showed HSF1 low expression (median: 136.0 months; $P = 0.004$, log-rank test) (Figure 5C). These findings suggest that overexpression of HSF1 was frequently observed in human HCCs, particularly in tumors exhibiting aggressive features.

To explore the pathological relationship between HSF1 and BAG3 in HCC samples, we performed immunohistochemical analysis for BAG3 in 226 HCC samples, which were also analyzed for HSF1 immunohistochemistry. The median percentage of positive cells was 25% (range: 0–85.0%) and we divided them into two groups—high expressers and low expressers—based on the percentage of BAG3-positive cells using a cutoff level of 25%, representing the median value of BAG3. Representative examples of immunohistochemical reactivity for BAG3 are shown in Figure 5B. Expressions of BAG3 protein were significantly increased in HCC specimens, whereas no or only low BAG3 expression was seen in adjacent non-cancerous tissue. BAG3 expression correlated significantly with histological grade ($P = 0.014$), and tumor size ($P = 0.035$), but no significant correlations were observed between BAG3 expression and other clinicopathological variables (Table I). Furthermore, a positive correlation between expressions of HSF1 and BAG3 was found in HCC ($P < 0.05$; Figure 5D) and patients with tumors showing BAG3 overexpression displayed significantly shorter overall survival (median: 84.0 months) compared with those patients whose tumors showed BAG3 low expression (median: 134.2 months; $P = 0.015$, log-rank test) (Figure 5E). Multivariate Cox regression

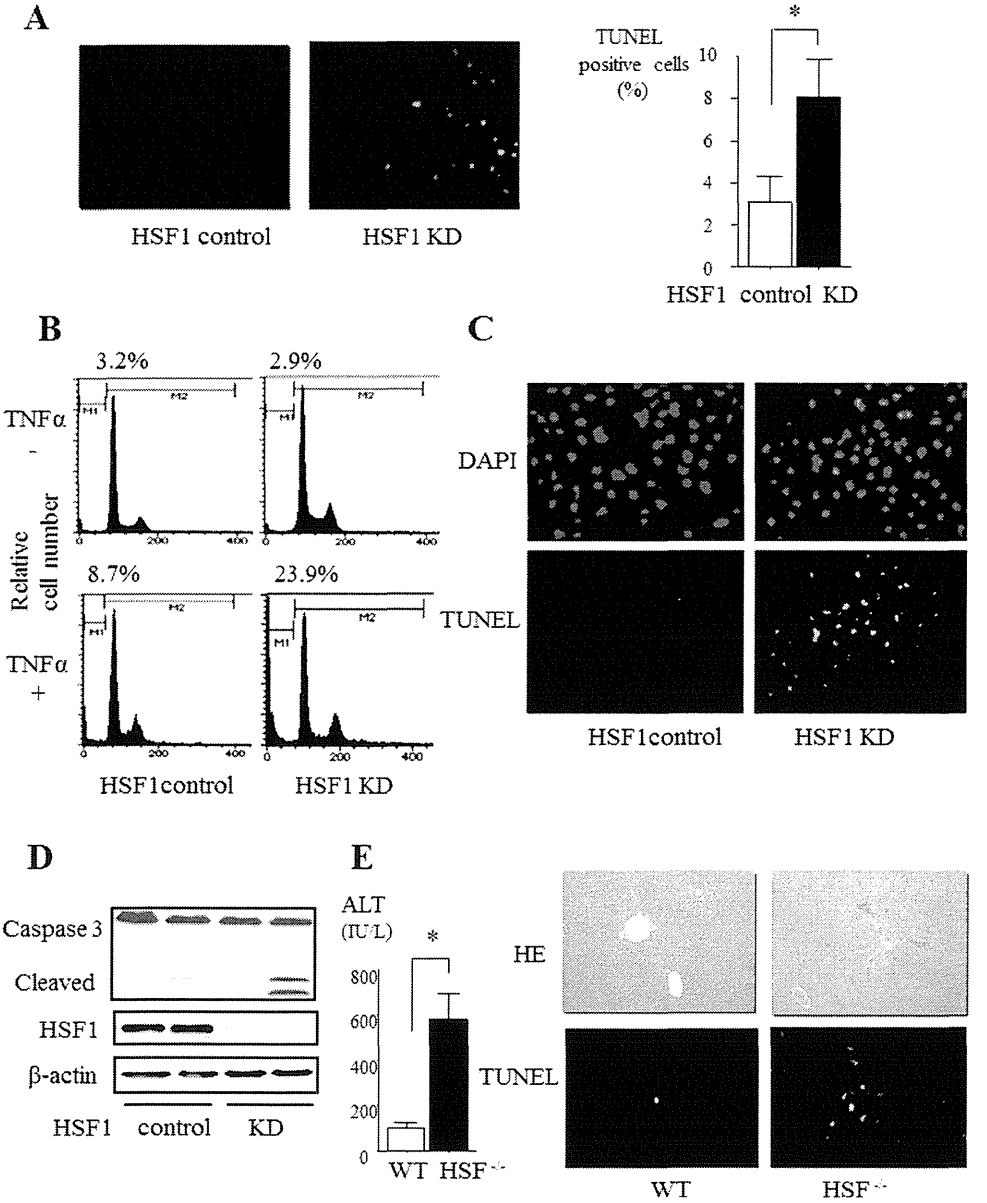

Fig. 3. Antiapoptotic effect of HSF1 in HCC cells and hepatocytes. (**A**) TUNEL staining was performed in tumors of HSF1 control and HSF1 KD cells from orthotopic implanted mice (left panel). TUNEL-positive cells were counted in tumors of HSF1 control and HSF1 KD cells. $^*P < 0.05$. Bars: SEM (right panel). (**B**) Apoptotic cells were evaluated by FACS at 24 h after incubation with TNF-α (30 ng/ml). Values indicate percentages of cells with sub-G_1 DNA content. Representative data are shown from three independent experiments. (**C**) TUNEL staining was performed in HSF1 control and KD cells after incubation with TNF-α. (**D**) Protein expressions of caspase 3, HSF1 and β-actin in TNF-α-treated HSF1 control and KD cells were determined by western blot analysis. (**E**) Serum ALT levels 7 h after injection of WT and HSF1$^{-/-}$ mice with LPS (5 μg/kg) and GalN (500 mg/kg). $^*P < 0.05$, compared with WT mice (left panel). HE and TUNEL stainings were performed in sections of livers obtained 7 h after injecting LPS (5 μg/kg) and GalN (500 mg/kg) into WT and HSF1$^{-/-}$ mice (right panel). ALT, alanine aminotransferase; DAPI, 4′,6-diamidino-2-phenylindole; HE, hematoxylin and eosin.

analysis identified high HSF1 expression (hazard ratio: 2.07; $P = 0.04$) as an independent prognostic factor for overall survival (Table II).

Discussion

As a master regulator of the heat shock response, HSF1 enhances organism survival and longevity in the face of environmental challenges. However, HSF1 can also act to the detriment of organisms by supporting malignant transformation (34). As reported previously, loss of HSF1 negatively impacts tumorigenesis driven by p53 or Ras mutations (8,16). Since HSF1 does not act as a classic oncogene, the increased resistance to proteotoxic stress induced by HSF1 was suggested to support tumor initiation and growth by enabling cells to accommodate the genetic alterations that accumulate during malignancy (35). However, the specific mechanisms by which HSF1 may support the growth of tumors are not well understood. Here, we have demonstrated that HSF1 has detrimental effects on liver tumor growth. We also proposed that the antiapoptotic effect of HSF1 may play a role in HCC tumor growth.

To clarify the mechanisms underlying this effect, we investigated associations between HSF1 and the NF-κB signaling pathway. Although, in a previous study, heat shock blocked the degradation of IκB (36) and nuclear translocation of NF-κB, the recent literature has reported that the presence of constitutively active HSF1 does not block TNF-α-induced activation of the NF-κB pathway or expression of a set of NF-κB-dependent genes (37). The current study established HSF1 KD cells and showed that HSF1 was necessary for TNF-α-induced NF-κB activation. We analyzed the function of BAG3 as a candidate for the molecule connecting HSF1 with NF-κB activation. BAG3 has reportedly been characterized by the

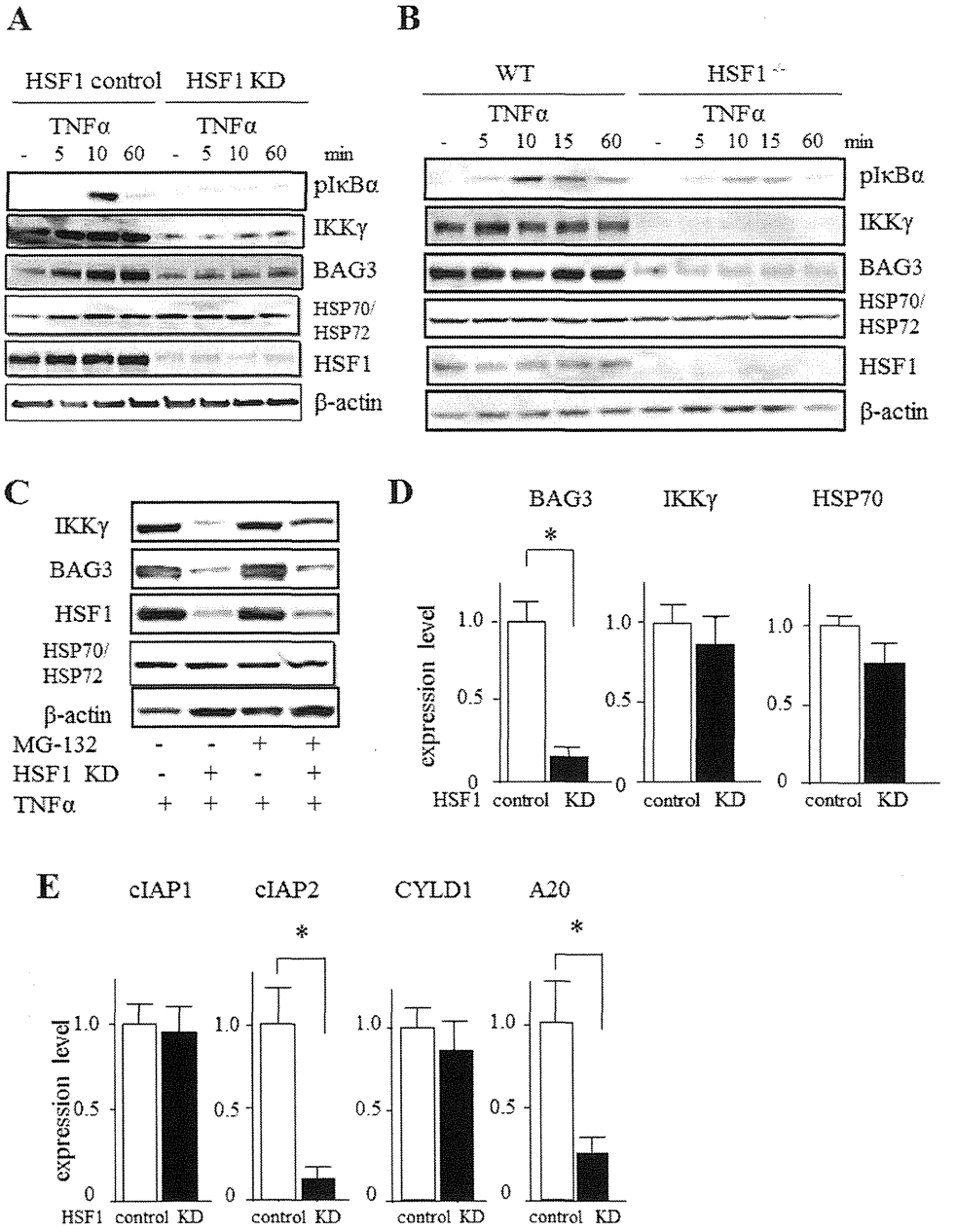

Fig. 4. HSF1 is involved in TNF-α-mediated NF-κB activation. (**A**) HSF1 control and KD cells were treated with TNF-α (30 ng/ml), lysed at the indicated times, gel separated and immunoblotted with antibodies against the indicated proteins. (**B**) HSF1 WT and HSF$^{-/-}$ hepatocytes treated with TNF-α (30 ng/ml), lysed at the indicated times, gel separated and immunoblotted with antibodies against the indicated proteins. (**C**) HSF1 control and KD cells were treated with TNF-α (30 ng/ml) with or without MG-132, lysed at 24 h, gel separated and immunoblotted with antibodies against indicated proteins. (**D**) Relative mRNA levels for BAG3, IKKγ and HSP70 in HSF1 control and KD cells determined by real-time PCR. Data are expressed as mean ± SEM (n = 4 per group). *P < 0.05. Bars: SEM. (**E**) Relative mRNA levels for antiapoptosis-related gene in HSF1 control and KD cells as determined by real-time PCR. Data are expressed as mean ± SEM (n = 4 per group). *P < 0.05. Bars: SEM. CYLD, cylindromatosis.

interaction with a variety of partners (Raf-1, steroid hormone receptors and HSP70) and is involved in regulating a number of cellular processes, particularly those associated with antiapoptosis (38). This molecule was expressed in response to stressful stimuli in a number of normal cell types and appears constitutively in a variety of tumors (33,39), and gene expression is regulated by HSF1 (40). In addition, knockdown of BAG3 protein decreased IKKγ levels, increasing tumor cell apoptosis and inhibiting tumor growth (33). Based on these considerations, we investigated whether attenuating HSF1 would enhance IKKγ protein expression, and data with MG-132 show that proteasomal degradation of IKKγ is enhanced in HSF1 KD cells. In addition, knowledge of the role BAG3 plays in preventing the proteasomal turnover of certain proteins suggests that the loss of BAG3 in HSF1 KD cells may be responsible for the enhanced turnover of IKKγ in this setting.

NF-κB activation is a master regulatory step in antiapoptosis. Several mechanisms have been reported regarding this antiapoptotic effect of NF-κB activation (41). NF-κB exerts its prosurvival activity primarily through the induction of target genes, the products of which inhibit components of the apoptotic machinery. These include Bcl-X_L and c-IAP (41), which binds directly to and inhibits the effect of caspases. This study showed that inactivation of NF-κB promoted apoptotic effects against TNF-α in HSF1$^{-/-}$ hepatocytes and HSF1 KD HCC cells. Real-time PCR analyses indicated that expression levels of apoptosis-related genes such as A20 and c-IAP2 were decreased by inhibition of NF-κB activation, whereas apoptosis-related genes such

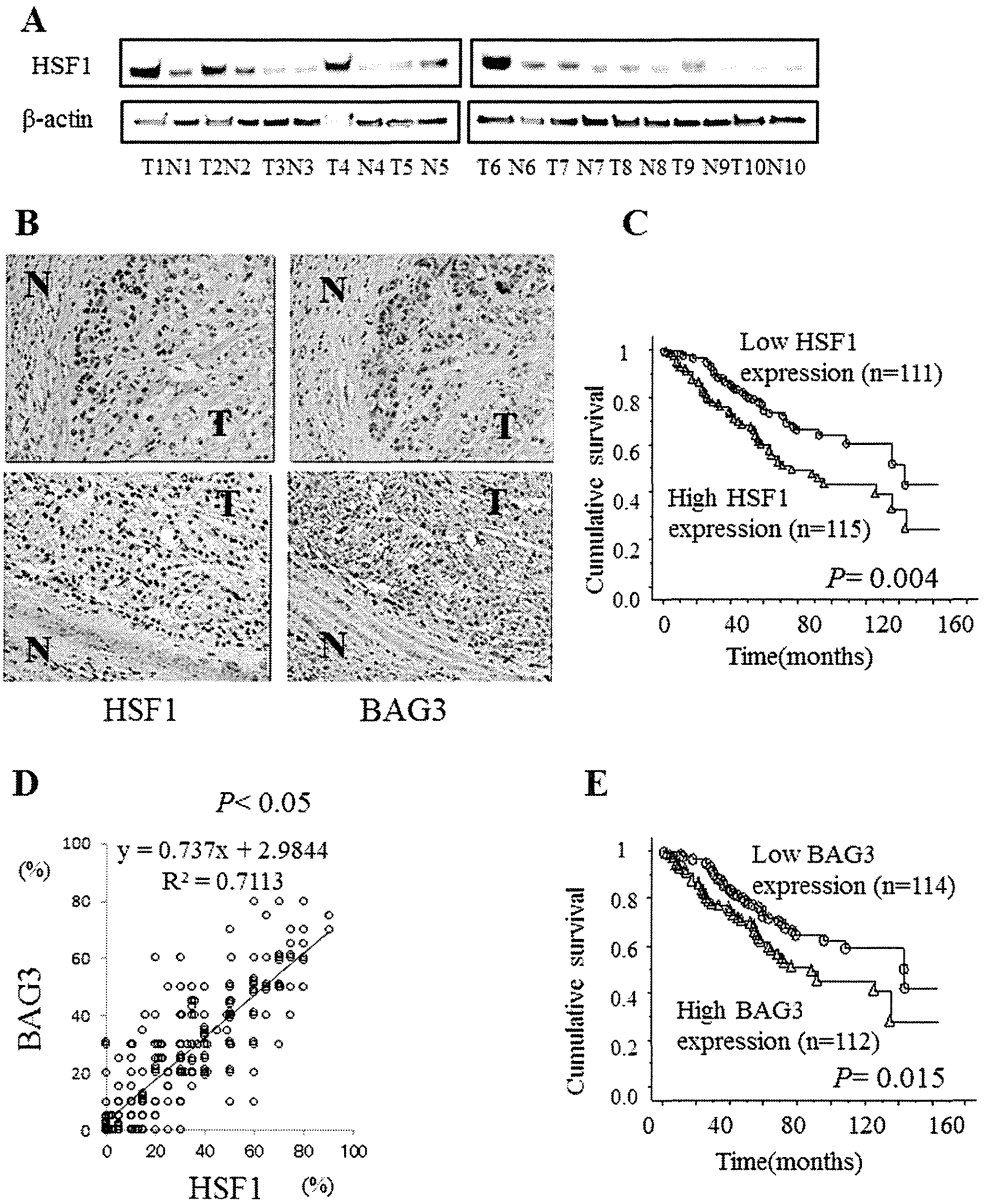

Fig. 5. Overexpression of HSF1 protein in human HCCs and pathological relationship between HSF1 and BAG3 in HCC samples. (**A**) HSF1 protein expression was determined in paired samples of human non-neoplastic liver and HCC by western blot, using β-actin as a control. N, non-cancerous liver; T, tumor. (**B**) Representative HSF1 and BAG3 staining of HCC and surrounding tissue. (**C**) Correlation of HSF1 overexpression with overall survival rates of patients. (**D**) Relationship between BAG3 and HSF1 expression in HCC. Scatterplot of BAG3 versus HSF1 with regression line displaying a correlation according to Spearman's correlation coefficient ($P < 0.01$). (**E**) Correlation of BAG3 overexpression with overall survival rates of patients.

as cIAP1 and cylindromatosis, which are known to be regulated by NF-κB activation, were apparently unaffected. Whether gene expression regulated by NF-κB activity differs between inducible and basal activation remains to be determined.

Regarding the relationship between HSF1 and HCC development, HSF1-deficient mice recently revealed dramatically reduced numbers and sizes of tumors compared with WT controls when tumors were induced by the chemical carcinogen, diethylnitrosamine. The same study suggested that the presence of extensive pathology associated with severe steatosis by diethylnitrosamine was prevented by HSF1 deletion and may be associated with reduced HCC development (42). On the other hand, ablation of IKKγ in liver parenchymal cells caused spontaneous development of HCC in mice, with tumor development preceded by steatohepatitis (43). Based on these observations, we assume that reductions in diethylnitrosamine-induced HCC development among HSF1-deficient mice may be associated with reduced expression of IKKγ, the reduction of which caused the steatosis.

BAG3 is a critical regulator of apoptosis in HSF1-deficient hepatocytes and HSF1 KD HCC cells. Moreover, the relationship between HSF1 and BAG3 has been shown not only in cell cultures and mouse models, but also in human HCC tissue samples; a correlation between HSF1 expression and BAG3 expression was found in HCC. Clinicopathological features and biological results provide a mechanistic link between HSF1 and HCC development via BAG3.

As for the ERK signal, a previous study demonstrated that impairment of JNK and ERK signaling in $HSF1^{-/-}$ MEF cells was caused in part by the reduced expression of EGFR (33). We showed a slight decrease in expression of EGFR among HSF1-deficient hepatocytes and HSF1 KD cells. On the other hand, the level of reduced activation of ERK, as a downstream molecule of EGFR, was larger than expected. However, the detailed mechanisms by which HSF1 regulates MAPK need further investigation.

In conclusion, we found that HSF1 deficiency significantly diminished NF-κB and MAPK activation in HCC hepatocytes and